Exciton-phonon system on a star graph: A perturbative approach

Saad Yalouz and Vincent Pouthier*
Institut UTINAM, Université de Franche-Comté, CNRS UMR 6213, 25030 Besançon Cedex, France
(Received 1 March 2016; published 9 May 2016)

Based on the operatorial formulation of the perturbation theory, the properties of an exciton coupled with optical phonons on a star graph are investigated. Within this method, the dynamics is governed by an effective Hamiltonian, which accounts for exciton-phonon entanglement. The exciton is dressed by a virtual phonon cloud whereas the phonons are clothed by virtual excitonic transitions. In spite of the coupling with the phonons, it is shown that the energy spectrum of the dressed exciton resembles that of a bare exciton. The only differences originate in a polaronic mechanism that favors an energy shift and a decay of the exciton hopping constant. By contrast, the motion of the exciton allows the phonons to propagate over the graph so that the dressed normal modes drastically differ from the localized modes associated to bare phonons. They define extended vibrations whose properties depend on the state occupied by the exciton that accompanies the phonons. It is shown that the phonon frequencies, either red shifted or blue shifted, are very sensitive to the model parameter in general, and to the size of the graph in particular.

DOI: 10.1103/PhysRevE.93.052306

I. INTRODUCTION

Exploiting the propagation of an elementary excitation in a molecular network is a promising way for performing scalable quantum computing [1]. For instance, in a dendrimer, that is a polymer whose hyperbranched structure looks like the fractal patterns that occur in the plant kingdom [2], the delocalization of an electronic exciton defines a physical realization of a continuous time quantum walk (CTQW) [3]. Extensively studied during the past few years, CTQW has become a very popular research subject due to its potential use in quantum information processing [4–6]. For example, a CTQW on a complex network provides a natural way for performing efficient quantum searches in the spirit of the well-known Grover's algorithm [7–9]. In that context, CTQW and exciton dynamics have been characterized in a great variety of networks including extended dendrimers [10,11], binary and glued trees [12,13], Apollonian networks [14,15], fractal networks [16,17], sequentially growing networks [18], and star graphs [19–24], to cite but a few examples. Similarly, the exciton propagation in molecular lattices may be used for performing high-fidelity quantum-state transfer (QST) at nanoscale. In quantum computing, QST is a fundamental task required to ensure an ideal communication between the elements of a computer or between adjacent computers [25]. Since the seminal work of Bose on Heisenberg ferromagnets [26], special attention has been paid for characterizing spin-excitation-mediated QST. Different systems were considered such as unmodulated spin chains and complex networks [27], spin chains with preengineered interactions [28–30], parallel spin chains [31], and time-dependent disordered chains [32]. But the spin degrees of freedom are not the only ones that can be used to promote QST and many alternatives were proposed such as phonons in crystals with reduced dimensionality [33–35] and vibrons in molecular chains [36,37].

In that context, when one considers exciton-mediated CTQW or QST in realistic systems, we face a major problem because the exciton does not propagate freely anymore. Instead, it interacts with the remaining degrees of freedom of the medium that usually form a phonon bath. The phonons are thus responsible for quantum decoherence [38–40], the public enemy number one in quantum computing. However, the physics of the decoherence strongly depends on the size of the network. In an infinite lattice, the phonons behave as a reservoir insensitive to the exciton [41] and the Born-Markov approximation is legitimate. Consequently, the exciton dynamics is well described using a generalized master equation (GME) that accounts for the irreversible decay of the coherence [42]. By contrast, in finite-size chains, the phonons no longer behave as a reservoir [43]. The Born-Markov approximation fails to capture the exciton dynamics and the GME approach breaks down [44].

To overcome this problem for the exciton-phonon system, we have introduced a method based on the operatorial formulation of the perturbation theory (PT) [45–48]. Within PT, the dynamics is governed by an effective Hamiltonian that takes exciton-phonon entanglement into account: the exciton get clothed by a virtual phonon cloud and the phonons are dressed by virtual excitonic transitions. In that case, quantum decoherence is encoded in the decoherence function [39,40] that provides information on the ability of the phonons to evolve freely in spite of the exciton-phonon coupling. At zero temperature, the phonons are in a pure state. The decoherence function reduces to a phase factor involving the frequency difference between free and dressed phonons. At finite temperature, an average procedure yields a sum over the phase factors, which interfere with the others, resulting in the decay of the excitonic coherences.

The previous scenario reveals that exciton-phonon interaction-induced phonon frequency shift is a key ingredient for understanding quantum decoherence. However, our previous works were restricted to linear chains. Therefore, in the present paper, the PT formalism is generalized for describing the Holstein model on a star graph, that is the coupling between an exciton and a set of optical phonons [49]. The star graph is one of the most regular structures in graph theory. Organized around a central core, it exhibits the local

*vincent.pouthier@univ-fcomte.fr

tree structure of irregular and complex networks. However, its topology remains sufficiently simple so that analytical calculations can be carried out.

The present work can thus be viewed as a first step where PT is applied for describing both the exciton energy corrections and the phonon frequency shifts. According to previous theories [45–48], this step is required for describing phonon-induced excitonic decoherence in a star graph, a phenomena whose the physics will be investigated in forthcoming papers.

The paper is organized as follows. In Sec. II, the star graph is introduced and the exciton-phonon Hamiltonian is established. Then, PT is applied to partially remove the exciton-phonon interaction and to derive the general expression of the exciton-phonon effective Hamiltonian. In Sec. III, the corresponding exciton energy corrections and dressed phonon normal modes are defined and studied numerically. The obtained results are discussed and interpreted, with a special emphasis on the influence of the size of the network.

II. THEORETICAL BACKGROUND

A. Exciton-phonon Hamiltonian

The star graph S_N we consider is shown in Fig. 1. It corresponds to a tree that involves N branches that emanate out from a central core. The central core, labeled by the index $\ell = 0$, is connected to N branch sites $\ell = 1, \ldots, N$. Each site ℓ is occupied by a molecular subunit whose internal (i.e., electronic or vibrational) dynamics is described by a two-level system. Let ω_0 denote the corresponding Bohr frequency and let $|\ell\rangle$ stand for the state in which the ℓth two-level system occupies its first excited state, the other two-level systems remaining in their ground state. The vacuum state $|\oslash\rangle$ describes all the two-level systems in their ground state.

Within these notations, the exciton Hamiltonian that governs the zero- and the one-exciton dynamics is defined as (with the convention $\hbar = 1$)

$$H_A = \sum_{\ell=0}^{N} \omega_0 |\ell\rangle\langle\ell| + \sum_{\ell=1}^{N} \Phi(|0\rangle\langle\ell| + |\ell\rangle\langle 0|), \tag{1}$$

where Φ is the exciton hopping constant. Because H_A is invariant under the discrete rotation of angle $\theta_0 = 2\pi/N$ and centered on the core site $\ell = 0$, its diagonalization is greatly simplified when one works with the so-called Bloch basis that

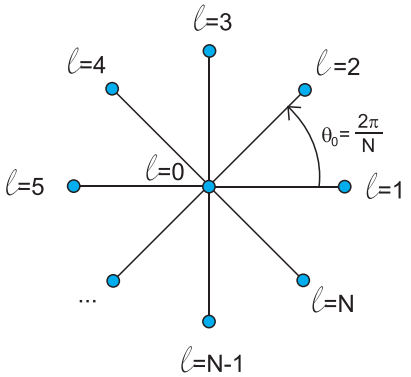

FIG. 1. Representation of the star graph S_N with $N + 1$ nodes $\ell = 0, \ldots, N$ and N branches.

involves the local state $|\ell = 0\rangle$ and N orthogonal Bloch states $|\psi_k\rangle$ $(k = 1, \ldots, N)$ defined as

$$|\psi_k\rangle = \frac{1}{\sqrt{N}} \sum_{\ell=1}^{N} e^{ik\ell\theta_0} |\ell\rangle. \tag{2}$$

In the Bloch basis, S_N supports two kinds of eigenstates. First, its spectrum shows the $(N-1)$-fold degenerate eigenenergy $\epsilon_k = \omega_0$, $\forall k = 1, \ldots, N-1$, the corresponding eigenstates being the $N-1$ Bloch states $|\chi_k\rangle = |\psi_k\rangle$, with $k = 1, \ldots, N-1$. Second, the graph supports two eigenstates $|\chi_0\rangle$ and $|\chi_N\rangle$ that correspond to superimpositions involving the core state $|0\rangle$ and the Bloch state $|\psi_N\rangle$ that is uniformly distributed over the periphery of the star. These totally symmetric eigenstates are defined as

$$|\chi_0\rangle = \frac{1}{\sqrt{2}}(|0\rangle - |\psi_N\rangle) \quad |\chi_N\rangle = \frac{1}{\sqrt{2}}(|0\rangle + |\psi_N\rangle), \tag{3}$$

the corresponding eigenenergy being $\epsilon_0 = \omega_0 - \sqrt{N}\Phi$ and $\epsilon_N = \omega_0 + \sqrt{N}\Phi$. Within these notations, the exciton Hamiltonian, that acts in the Hilbert space $\mathcal{E}_A$ whose dimension is equal to $N + 2$, is rewritten as

$$H_A = \sum_{k=0}^{N} \epsilon_k |\chi_k\rangle\langle\chi_k|. \tag{4}$$

Note that, here, we only accounts on the rotational symmetric of the star graph because we intent to describe realistic branched molecules that share this symmetry owing to couplings between neighboring branches (dendrimers, molecular wheels, etc.). However, under the present form, the star graph exhibits a stronger symmetry since it remains invariant under the permutation of its branches. This property can thus be exploited easily for defining a different set of eigenvectors to generate the entire subspace connected to the degenerate eigenenergy.

The exciton interacts with the external motions of the lattice, which are described by $N + 1$ independent oscillators localized on each site of the graph and with frequency Ω_0. These oscillators form a set of optical phonons whose Hamiltonian acts in the Hilbert space $\mathcal{E}_B$. This Hamiltonian is defined in terms of the standard phonon operators $a_\ell^\dagger$ and a_ℓ as

$$H_B = \sum_{\ell=0}^{N} \Omega_0 a_\ell^\dagger a_\ell. \tag{5}$$

According to the potential deformation model [50], the exciton-phonon interaction results from a random modulation of each exciton local state energy induced by the lattice vibrations. It is defined as

$$V = \sum_{\ell=0}^{N} M^{(\ell)}(a_\ell^\dagger + a_\ell), \tag{6}$$

where $M^{(\ell)} = \Delta_0 |\ell\rangle\langle\ell|$ is expressed in terms of the exciton-phonon coupling strength Δ_0. Acting in $\mathcal{E}_A$ only, $M^{(\ell)}$ is diagonal in the local basis $\{|\ell\rangle\}$, the ℓth element representing the influence of the ℓth optical phonon on the ℓth two-level Bohr frequency. By contrast, in the exciton eigenbasis $\{|\chi_k\rangle\}$,

$M^{(\ell)}$ is no longer diagonal. Its elements are defined as

$$M^{(\ell)}_{kk'} = \Delta_0 \chi^*_{k\ell}\chi_{k'\ell}, \tag{7}$$

where $\chi_{k\ell} = \langle \ell|\chi_k\rangle$ is the exciton wave function.

On the star graph, the exciton-phonon system is governed by the Hamiltonian $H = H_0 + V$ where $H_0 = H_A + H_B$ is the unperturbed Hamiltonian. Since H conserves the exciton number, the Hilbert space $\mathcal{E} = \mathcal{E}_A \otimes \mathcal{E}_B$ is partitioned into independent subspaces as $\mathcal{E} = \mathcal{E}_0 \oplus \mathcal{E}_1$. In the zero-exciton subspace $\mathcal{E}_0$, $V = 0$ so that the unperturbed states are eigenstates of H. They correspond to tensor products involving the vacuum $|\varnothing\rangle$ and the phonon number states $|\{n_\ell\}\rangle = |n_1,\ldots,n_N\rangle$. They describe n_ℓ free phonons with energy $n_\ell\Omega_0$ localized on each site ℓ. In the one-exciton subspace $\mathcal{E}_1$, the unperturbed states $|\chi_k\rangle \otimes |\{n_\ell\}\rangle$ refer to free phonons accompanied by an exciton in state $|\chi_k\rangle$. Since V turns on in $\mathcal{E}_1$, they are no longer eigenstates of H. The exact eigenstates are entangled exciton-phonon states that result from transitions, which mix both exciton and phonon degrees of freedom. Indeed, V yields exciton transitions from $|\chi_k\rangle$ with energy ϵ_k, to $|\chi_{k'}\rangle$ with energy $\epsilon_{k'}$, via the exchange of a phonon ℓ with energy Ω_0. The allowed transitions are specified by the selection rules $M^{(\ell)}_{kk'} \neq 0$.

In the following of the text, we shall restrict our attention to the so-called nonadiabatic weak-coupling limit : $\omega_0 \gg \Omega_0$ (high-energy exciton), $4\sqrt{N}\Phi < \Omega_0$ (nonadiabatic limit) and $\Delta_0 \ll \Phi$ (weak-coupling limit). In that case, there is no resonance between coupled unperturbed states since $\epsilon_k - \epsilon_{k'} \neq \pm\Omega_0$. Consequently, within the weak-coupling limit, second-order PT can be applied to treat the influence of the coupling V, as detailed in the next section. Note that alternative procedures can be used to consider the nonadiabatic strong-coupling limit by combining PT with a Lang-Firsov transformation [47,48].

B. Perturbation theory

In its operatorial formulation [51], PT is based on the introduction of a unitary transformation that provides a new point of view in which the exciton-phonon dynamics is described by an effective Hamiltonian. The key point is that this Hamiltonian is diagonal in the unperturbed basis. Quite powerful to treat finite-size chains [36,37,45,46], this approach breaks down for the star graph because the unperturbed Hamiltonian exhibits quasidegenerate states.

To illustrate this feature, let us consider the two states $|\chi_k\rangle \otimes |n_1,\ldots,n_\ell,\ldots,n_N\rangle$ and $|\chi_{k'}\rangle \otimes |n_1-1,\ldots,n_\ell+1,\ldots,n_N\rangle$. Since they refer to the same phonon number $N_{\rm ph} = n_1 + ,\ldots,n_\ell + ,\ldots,n_N$, they have exactly (or almost) the same energy. Of course, these states do not directly interact through the coupling V because they share the same phonon number. However, through phonon exchanges, they may be coupled with a same unperturbed state, such as for example $|\chi_{k''}\rangle \otimes |n_1,\ldots,n_\ell+1,\ldots,n_N\rangle$. As a consequence, an effective coupling occurs between these exactly degenerate (or quasidegenerate) states resulting in errors in the calculations of the corrected energies and in divergences in the evaluation of the entangled exciton-phonon states.

To overcome this problem, quasidegenerate PT is applied [52] (Appendix). To proceed, we take advantage of the fact that the effective couplings conserve the phonon number. Therefore, our procedure involves a transformation $U = \exp(S)$ that generates a new point of view in which the effective Hamiltonian $\hat{H} = UHU^\dagger$ is block diagonal in the unperturbed basis. The generator S is expanded as a Taylor series in the coupling V so that $\hat{H}$ becomes a phonon conserving operator. Up to second order, it is written as

$$\hat{H} = H_A + \delta H_A + \sum_{\ell=0}^{N}\sum_{\ell'=0}^{N}[\Omega_0\delta_{\ell\ell'} + \Lambda(\ell\ell')]a^\dagger_\ell a_{\ell'}, \tag{8}$$

where δH_A and $\Lambda(\ell\ell')$ are operators in $\mathcal{E}_A$ whose matrix elements are defined as (in the unperturbed basis $\{|\chi_k\rangle\}$)

$$\begin{aligned}
\delta H_{Ak_1k_2} &= \frac{1}{2}\sum_{\ell=0}^{N}\sum_{k=0}^{N}\frac{M^{(\ell)}_{k_1k}M^{(\ell)}_{kk_2}}{\epsilon_{k_1}-\epsilon_k-\Omega_0} + \frac{M^{(\ell)}_{k_1k}M^{(\ell)}_{kk_2}}{\epsilon_{k_2}-\epsilon_k-\Omega_0}\\
\Lambda(\ell\ell')_{k_1k_2} &= \frac{1}{2}\sum_{k=0}^{N}\frac{M^{(\ell)}_{k_1k}M^{(\ell')}_{kk_2}}{\epsilon_{k_1}-\epsilon_k+\Omega_0} + \frac{M^{(\ell')}_{k_1k}M^{(\ell)}_{kk_2}}{\epsilon_{k_2}-\epsilon_k-\Omega_0}\\
&\quad + \frac{1}{2}\sum_{k=0}^{N}\frac{M^{(\ell')}_{k_1k}M^{(\ell)}_{kk_2}}{\epsilon_{k_1}-\epsilon_k-\Omega_0} + \frac{M^{(\ell)}_{k_1k}M^{(\ell')}_{kk_2}}{\epsilon_{k_2}-\epsilon_k+\Omega_0}.
\end{aligned} \tag{9}$$

δH_A defines the correction of the exciton Hamiltonian owing to the coupling with the phonons. It results from the spontaneous emission of a phonon during which the exciton realizes a transition from $|\chi_{k_1}\rangle$ to $|\chi_k\rangle$. However, in the non adiabatic limit, the energy is not conserved during the transition. The emitted phonon is immediately reabsorbed and the exciton realizes a second transition from $|\chi_k\rangle$ to $|\chi_{k_2}\rangle$. In other words, the exciton does no longer propagate freely and it is as if it were dressed by a virtual phonon cloud. This dressing renormalizes the exciton energies ϵ_k by an amount $\delta\epsilon_k = \delta H_{Akk}$. In addition, it induces effective interactions $\delta H_{Ak_1k_2}$ between distinct unperturbed states that can no longer be neglected for quasidegenerate states.

Similarly, $\Lambda(\ell\ell')$ defines the so-called phonon hopping constant matrix that accounts for the correction of the phonon Hamiltonian. It has two origins. First, a phonon can be absorbed on a particular site ℓ giving rise to excitonic transition. Because this transition does not conserve the energy, the phonon is immediately reemitted but on another site ℓ'. Second, a phonon localized on a site ℓ can favor the stimulated emission of a second phonon during which the exciton realizes a transition. But, as previously, the emitted phonon is immediately reabsorbed, but on a second site ℓ'. Both mechanisms are virtual processes indicating that the phonons are dressed by virtual transitions realized by the exciton. As a result, correlations between sites occur so that the dressed phonons become able to delocalize over the star graph.

III. RESULTS AND DISCUSSION

In this section, the previous formalism is applied for describing the exciton energy corrections and the dressed phonon normal modes induced by the exciton-phonon interaction. To proceed, reduced parameters will be used [53]. First, the adiabaticity will be measured by the standard parameter $B = 2\Phi/\Omega_0$. Nevertheless, to account for the specificity of the star graph, we shall introduce the N-dependent adiabaticity

$B_N = 2\Phi\sqrt{N}/\Omega_0 = \sqrt{N}B$. The exciton-phonon coupling strength will be measured by the reduced parameter $C = \Delta_0/\Omega_0$. It is related to the so-called small polaron binding energy $E_B = \Delta_0^2/\Omega_0$ according to the relation $C^2 = E_B/\Omega_0$.

A. Quantum states of the dressed exciton

According to the previous formalism, the dynamics of a dressed exciton is governed by the effective Hamiltonian $\hat{H}_A = H_A + \delta H_A$ whose eigenvalues $\hat{\epsilon}_k$, with $k = 0, \ldots, N$, define the corrected exciton energies. In the unperturbed eigenbasis $\{|\chi_k\rangle\}$, δH_A is expressed as,

$$\delta H_A = \begin{pmatrix} \delta\epsilon_0 & 0 & 0 & \ldots & \delta h \\ 0 & \delta\epsilon_1 & 0 & \ldots & 0 \\ 0 & 0 & \delta\epsilon_2 & \ldots & 0 \\ \ldots & \ldots & \ldots & \ldots & \ldots \\ \delta h & 0 & 0 & \ldots & \delta\epsilon_N \end{pmatrix}, \tag{10}$$

where the different parameters are defined as

$$\begin{aligned} \delta\epsilon_0 &= -E_B\frac{N+1}{4N}\left(1+\frac{1}{1+B_N}+\left(\frac{N-1}{N+1}\right)\frac{4}{2+B_N}\right) \\ \delta\epsilon_k &= -\frac{E_B}{N}\left(N-1+\frac{4}{4-B_N^2}\right) \quad \forall k = 1,\ldots,N-1 \\ \delta\epsilon_N &= -E_B\frac{N+1}{4N}\left(1+\frac{1}{1-B_N}+\left(\frac{N-1}{N+1}\right)\frac{4}{2-B_N}\right) \\ \delta h &= -E_B\frac{N-1}{8N}\left(2+\frac{2}{1-B_N^2}-\frac{16}{4-B_N^2}\right). \end{aligned} \tag{11}$$

From Eqs. (10) and (11), the effective Hamiltonian $\hat{H}_A$ can be diagonalized quite straightforwardly. The resulting eigenvalues are shown in Fig. 2 that displays the influence of the exciton-phonon coupling on the energy spectrum for different N values. It turns out that the coupling with the phonons have two main effects on the excitonic spectrum. First, in the new point of view, the Bloch states $\{|\chi_k\rangle\}$ with $k = 1, \ldots, N-1$ still define $N-1$ eigenstates of the transformed Hamiltonian $\hat{H}_A$. However, the corresponding eigenenergies are red shifted by an amount $\delta\epsilon_k$ that is k independent [see Eq. (11)]. Consequently, the coupling preserves the degeneracy of the spectrum that still supports the $(N-1)$-fold degenerate energy, a characteristic of the spectrum of a bare exciton. This degenerate energy level is almost N independent and it exhibits a red shift that shows a quadratic dependence with the coupling strength C. Then, the second effect of the exciton-phonon interaction is to couple the two states $|\chi_0\rangle$ and $|\chi_N\rangle$ through the parameter δh [see Eq. (10)]. Consequently, the spectrum exhibits two discrete energy levels that refer to dressed states which correspond *a priori* to superimpositions involving $|\chi_0\rangle$ and $|\chi_N\rangle$. After simple algebraic manipulations, these energy levels are defined as

$$\begin{aligned} \hat{\epsilon}_0 &= \frac{\bar{\epsilon}_N+\bar{\epsilon}_0}{2} - \sqrt{\left(\frac{\bar{\epsilon}_N-\bar{\epsilon}_0}{2}\right)^2+\delta h^2} \\ \hat{\epsilon}_N &= \frac{\bar{\epsilon}_N+\bar{\epsilon}_0}{2} + \sqrt{\left(\frac{\bar{\epsilon}_N-\bar{\epsilon}_0}{2}\right)^2+\delta h^2}, \end{aligned} \tag{12}$$

where $\bar{\epsilon}_{N,0} = \epsilon_{N,0} + \delta\epsilon_{N,0}$. As shown in Fig. 2, the discrete energy levels are located on each side of the $(N-1)$-fold degenerate eigenenergy. However, their position strongly depends on the size of the graph. For $C = 0$, such a behavior originates in the N dependence of the energies of the bare states defined as $\omega_0 \pm \sqrt{N}\Phi$. For nonvanishing C values, in addition to this effect, a size dependence also occurs through the red shift that affects each discrete energy level [see Eq. (11)]. This shift is enhanced by the coupling and it varies according to a quadratic law with respect to C. Note that we have observed a band narrowing effect. As C increases, the two discrete energy levels become closer to each other, the energy difference scaling as $(\hat{\epsilon}_N - \hat{\epsilon}_0)/2\sqrt{N}\Phi \approx 1 - C^2$.

The behavior of the coupling δh between the nondegenerate states $|\chi_0\rangle$ and $|\chi_N\rangle$ is illustrated in Fig. 3 for $C = 0.01$. The

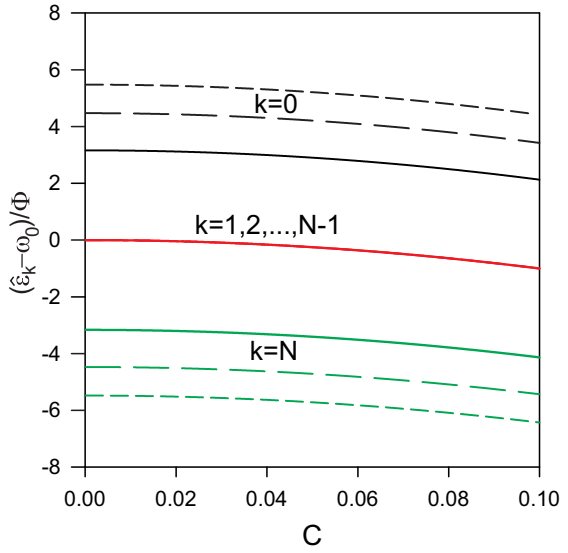

FIG. 2. Coupling dependence of the exciton energy spectrum for $B = 0.01$ and for $N = 10$ (full lines), $N = 20$ (long dashed lines) and $N = 30$ (short dashed lines).

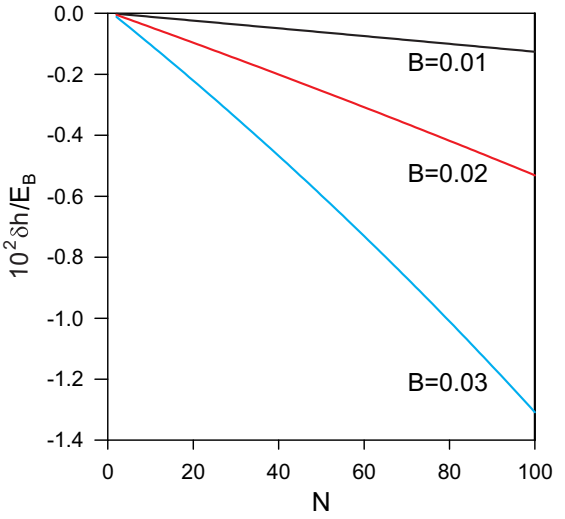

FIG. 3. Size dependence of the coupling δh between the nondegenerate eigenstates $|\chi_0\rangle$ and $|\chi_N\rangle$ for $C = 0.01$ and for $B = 0.01$, $B = 0.02$, and $B = 0.03$.

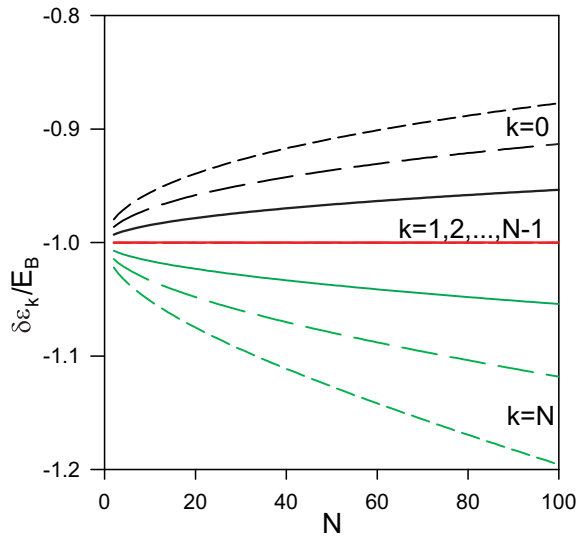

FIG. 4. Size dependence of the energy shifts $\delta\epsilon_k$ for $C = 0.01$ and for $B = 0.01$ (full lines), $B = 0.02$ (long dashed lines), and $B = 0.03$ (short dashed lines).

coupling δh decreases almost linearly with N, a decay that is enhanced by the adiabaticity. However, the key point concerns the strength of the coupling. For instance, for $B = 0.02$, δh evolves from $-4.5 \times 10^{-4} E_B$ for $N = 10$ to $-5.3 \times 10^{-3} E_B$ for $N = 100$. As a result, δh is approximately six orders of magnitude smaller than the difference $2\sqrt{N}\Phi$ between the energies of the states $|\chi_0\rangle$ and $|\chi_N\rangle$. This behavior is quite well captured by the Taylor expansion for small B values $\delta h \approx -(N-1)B^2 E_B/8$. Consequently, δh is an extremely small parameter that can be neglected in the calculations. The coupling between the unperturbed states $|\chi_0\rangle$ and $|\chi_N\rangle$ can be disregarded so that these states define approximately two eigenstates of the effective Hamiltonian.

Within this approximation, the effective Hamiltonian $\hat{H}_A$ becomes diagonal in the unperturbed basis $\{|\chi_k\rangle\}$, $\forall k = 0, \ldots, N$. Its eigenvalues reduce to the corrected unperturbed energies defined as

$$\begin{aligned} \hat{\epsilon}_0 &\approx \omega_0 - \sqrt{N}\Phi + \delta\epsilon_0 \\ \hat{\epsilon}_k &= \omega_0 + \delta\epsilon_k \quad \forall k = 1, \ldots, N-1 \\ \hat{\epsilon}_N &\approx \omega_0 + \sqrt{N}\Phi + \delta\epsilon_N. \end{aligned} \tag{13}$$

The influence of the size of the star on the energy shifts is displayed in Fig. 4 for a weak coupling $C = 0.01$ and for three values of the adiabaticity $B = 0.01$ (full lines), $B = 0.02$ (long dashed lines), and $B = 0.03$ (short dashed lines). The figure clearly shows that the order of magnitude of the energy shifts is about the small polaron binding energy E_B. However, different behaviors take place depending on the nature of the states. Indeed, the shift experienced by the energy of the $N-1$ degenerate Bloch states is basically independent on both the size of the star and the adiabaticity, provided that B remains sufficiently small. One thus obtains $\delta\epsilon_k \approx -E_B, \forall k = 1, \ldots, N-1$. By contrast, for the nondegenerate state $|\chi_0\rangle$, the energy shift slightly increases with both the size of the star and the adiabaticity. For instance, for $B = 0.01$, $\delta\epsilon_0$ varies from $-0.98E_B$ for $N = 10$ to $-0.95E_B$ for $N = 100$. Similarly, for $N = 50$, $\delta\epsilon_0$ increases from $-0.97E_B$ for $B = 0.01$ to $-0.91E_B$ for $B = 0.03$. The opposite behavior occurs for the state $|\chi_N\rangle$ whose energy shift slightly decreases when both the size of the star and the adiabaticity increase. For instance, for $B = 0.01$, $\delta\epsilon_N$ decreases from $-1.02E_B$ for $N = 10$ to $-1.05E_B$ for $N = 100$. Similarly, for $N = 50$, $\delta\epsilon_N$ varies from $-1.04E_B$ for $B = 0.01$ to $-1.13E_B$ for $B = 0.03$. Note that we have observed that the energy shift of the non degenerate states evolve almost linearly with B for small B values whereas a quadratic correction occurs for larger B values. Note that the different features observed in Figs. 4 are easily explained when one considers the Taylor expansion of the shifts in the non adiabatic limit. For small B values one obtains

$$\begin{aligned} \delta\epsilon_0/E_B &\approx -1 + \frac{\sqrt{N}}{2}B - \frac{3N+1}{8}B^2 \\ \delta\epsilon_k/E_B &\approx -1 - \frac{B^2}{4} \quad \forall k = 1, \ldots, N-1 \\ \delta\epsilon_N/E_B &\approx -1 - \frac{\sqrt{N}}{2}B - \frac{3N+1}{8}B^2. \end{aligned} \tag{14}$$

The previous results reveal that PT provides a new point of view in which the exciton dynamics is governed by the effective Hamiltonian $\hat{H}_A$ that is diagonal in the unperturbed basis $\{|\chi_k\rangle\}$. In this point of view, $|\chi_k\rangle$ defines a quantum state in which the exciton no longer evolves freely but is dressed by a virtual cloud of phonons. The corresponding energy $\hat{\epsilon}_k = \epsilon_k + \delta\epsilon_k$ exhibits a correction $\delta\epsilon_k$. It is a signature of the dressing mechanism whose parameter dependence can be interpreted using the small polaron theory [53,54]. Within this formalism, the dressing favors two main effects. First, it yields a red shift of the Bohr frequency of each two-level system equal to the small polaron binding energy. Then, it modifies the propagation of the exciton that delocalizes according to a reduced hopping constant $\hat{\Phi} = \Phi \exp(-S)$, where the band-narrowing factor at zero temperature is $S = E_B/\Omega_0$. As a result, the energy correction of the Bloch states scales as $\delta\epsilon_k \approx -E_B$, $\forall k = 1, \ldots, N-1$, as observed in Fig. 4. By contrast, for the discrete states whose energy depends on the hopping constant, an additional effect occurs. The corresponding energy shifts are defined as $\delta\epsilon_0 \approx -E_B + \sqrt{N}\Phi S$ and $\delta\epsilon_N \approx -E_B - \sqrt{N}\Phi S$, in a quite good agreement with the results obtained in Eq. (14).

B. Dressed phonon normal modes and phonon frequency shifts

In the previous section, we have shown that $\hat{H}_A$ behaves as a diagonal operator in the excitonic basis $\{|\chi_k\rangle\}$. At first glance, this is no longer the case for the effective exciton-phonon Hamiltonian Eq. (8). Couplings mediated by the phonon hopping constant matrix $\Lambda(\ell\ell')$ remain between the unperturbed states [see Eq. (9)]. However, our numerical analysis revealed that the phonon hopping constant matrix yields very small modifications of the exciton dynamics when compared with those induced by the energy corrections $\delta\epsilon_k$. As a result, up to second order in V, a quite good approximation consists in neglecting the nondiagonal part of these operators. Within this approximation, the effective exciton-phonon Hamiltonian can

be rewritten as

$$\hat{H} \approx \sum_{k=0}^{N} \hat{\epsilon}_k |\chi_k\rangle\langle\chi_k| + \hat{H}_B^{(k)} \otimes |\chi_k\rangle\langle\chi_k|, \tag{15}$$

where $\hat{H}_B^{(k)}$ is the Hamiltonian that governs the phonon dynamics when the exciton lies in the state $|\chi_k\rangle$. By setting $\Lambda_{\ell\ell'}^{(k)} = \Lambda(\ell\ell')_{kk}$, it is defined as

$$\hat{H}_B^{(k)} = \sum_{\ell=0}^{N}\sum_{\ell'=0}^{N} \left[\Omega_0\delta_{\ell\ell'} + \Lambda_{\ell\ell'}^{(k)}\right] a_\ell^\dagger a_{\ell'}. \tag{16}$$

According to Eq. (16), the influence of an exciton in a state $|\chi_k\rangle$ that accompanies the phonons is twofold. First, it favors a shift $\Lambda_{\ell\ell}^{(k)}$ of the frequency of each local oscillator $\ell = 0,\ldots,N$. Then, it provides a coupling $\Lambda_{\ell\ell'}^{(k)}$ between distinct local oscillators so that the dressed phonons become able to delocalize along the star graph. According to Eqs. (7) and (9), these couplings specify pathways for the phonon propagation whose nature is intimately connected to the overlaps between the excitonic wave functions involved in the virtual transitions that dress the phonons. As a result, the vibrational normal modes that define the dressed phonons are fully different from the localized normal modes associated to free phonons. These dressed normal modes are obtained from the diagonalization of the phonon hopping constant matrix $\Lambda^{(k)}$. Such a procedure allows us to define $N+1$ eigenvalues $\delta\Omega_q^{(k)}$ and $N+1$ eigenvectors $\beta_q^{(k)}(\ell)$ labeled by the index $q = 0,1,\ldots,N$. The index q refers to a particular phonon mode with energy $\Omega_q^{(k)} = \Omega_0 + \delta\Omega_q^{(k)}$, the eigenvalues of the phonon hopping constant matrix defining the phonon frequency shifts. The dynamics of each mode is described by the well-known creation $a_q^{(k)\dagger}$ and annihilation $a_q^{(k)}$ operators, written as

$$a_q^{(k)} = \sum_{\ell=0}^{N} \beta_q^{(k)*}(\ell) a_\ell \quad a_q^{(k)\dagger} = \sum_{\ell=0}^{N} \beta_q^{(k)}(\ell) a_\ell^\dagger. \tag{17}$$

Within the normal mode decomposition, the phonon Hamiltonian is finally rewritten in the standard form as

$$\hat{H}_B^{(k)} = \sum_q \Omega_q^{(k)} a_q^{(k)\dagger} a_q^{(k)}. \tag{18}$$

Note that to make the determination of the phonon normal modes easier, it is convenient to introduce an abstract linear vector space notation by considering the phonon operators a_ℓ as the components of the vector $|a\rangle$ in the local representation $\{|\ell\rangle\}$. Then, one introduces the operators $\Lambda^{(k)}$ and $\bar{\Omega}_0$ whose matrix elements are defined as $\Lambda_{\ell\ell'}^{(k)} = (\ell|\Lambda^{(k)}|\ell')$ and $\Omega_0\delta_{\ell\ell'} = (\ell|\bar{\Omega}_0|\ell')$, respectively. The normal modes are thus extracted from the eigenvalue equation associated to the operator $\Lambda^{(k)}$, as

$$\Lambda^{(k)}\big|\beta_q^{(k)}\big) = \delta\Omega_q^{(k)}\big|\beta_q^{(k)}\big), \tag{19}$$

where $|\beta_q^{(k)})$ denotes a column vector whose elements $\beta_q^{(k)}(\ell) = (\ell|\beta_q^{(k)})$ define the normal modes. Finally, within these notations, the phonon operators reduce to $a_q^{(k)} = (\beta_q^{(k)}|a)$ and $a_q^{(k)\dagger} = (a|\beta_q^{(k)})$ and the phonon Hamiltonian is rewritten as

$$\hat{H}_B^{(k)} = (a|[\bar{\Omega}_0 + \Lambda^{(k)}]|a). \tag{20}$$

At this step, let us mention that the nature of the dressed phonon normal modes is very sensitive to the state occupied by the exciton that accompanies the phonons. Two different situations occur depending on whether the exciton occupies a totally symmetric state $|\chi_{0,N}\rangle$ or a Bloch state $|\chi_k\rangle$, with $k = 1,\ldots,N-1$, as shown in the following of the text.

1. *Phonons dressed by an exciton occupying a totally symmetric state*

When the phonons are accompanied by an exciton that occupies a totally symmetric state $|\chi_k\rangle$ with $k = 0$ or N, the only elements of the phonon hopping constant matrix that contribute to the phonon dynamics are expressed as

$$\begin{aligned}
\Lambda_{00}^{(k)} &= -\alpha^{(k)} \\
\Lambda_{\ell 0}^{(k)} &= \Lambda_{0\ell}^{(k)} = \frac{\alpha^{(k)}}{N} \quad \forall \ell \neq 0 \\
\Lambda_{\ell\ell}^{(k)} &= -\frac{\alpha^{(k)} + (N-1)\gamma^{(k)}}{N^2} \quad \forall \ell \neq 0 \\
\Lambda_{\ell\ell'}^{(k)} &= \frac{\gamma^{(k)} - \alpha^{(k)}}{N^2} \quad \forall \ell \neq \ell' \neq 0,
\end{aligned} \tag{21}$$

where the parameters $\alpha^{(k)}$ and $\gamma^{(k)}$ are defined as

$$\begin{aligned}
\alpha^{(k)} &= \left(\frac{\delta_{kN} - \delta_{k0}}{2}\right)\frac{E_B B_N}{1 - B_N^2} \\
\gamma^{(k)} &= \left(\frac{\delta_{kN} - \delta_{k0}}{2}\right)\frac{4E_B B_N}{4 - B_N^2}.
\end{aligned} \tag{22}$$

Note that the phonon hopping constant matrix satisfies the relation $\sum_{\ell'} \Lambda_{\ell\ell'}^{(k)} = 0$.

From Eq. (21), a moment's reflection will convince the reader that the phonon hopping constant matrix corresponds to the adjacency matrix of a finite graph built from the combination between a star graph and a complete graph. As a result, this matrix is invariant under the discrete rotation of angle $\theta_0 = 2\pi/N$ and centered on the core site $\ell = 0$. Therefore, to make its diagonalization easier, it is convenient to work with the Bloch representation that involves the local vector $|\ell = 0)$ and N orthogonal Bloch vectors $|\psi_q)$ $(q = 1,\ldots,N)$ defined as

$$|\psi_q) = \frac{1}{\sqrt{N}} \sum_{\ell=1}^{N} e^{iq\ell\theta_0} |\ell). \tag{23}$$

In the Bloch representation, $\Lambda^{(k)}$ supports two kinds of eigenstates. First, its spectrum shows a $(N-1)$-fold degenerate eigenvalue $\delta\Omega_q^{(k)} = -\gamma^{(k)}/N$, $\forall q = 1,\ldots,N-1$. This phonon frequency shift is associated to $N-1$ normal modes that correspond to $N-1$ Bloch vectors $|\beta_q^{(k)}) = |\psi_q)$, with $q = 1,\ldots,N-1$. Such normal modes describe vibrations delocalized over the periphery of the star. This spatial dependence originates in the overlaps between the totally symmetric state occupied by the exciton that accompanies the phonons and the excitonic Bloch states that participate to the virtual transitions responsible for the dressing mechanism.

Second, the phonon hopping constant matrix exhibits two eigenstates $|\beta_0^{(k)})$ and $|\beta_N^{(k)})$ that are superimpositions involving the core vector $|0)$ and the Bloch vector $|\psi_N)$. These totally

symmetric normal modes are defined as

$$|\beta_0^{(k)}) = \sqrt{\frac{N}{N+1}}\left(|0) - \sum_{\ell=1}^{N}\frac{1}{N}|\ell)\right)$$
$$|\beta_N^{(k)}) = \frac{1}{\sqrt{N+1}}\left(|0) + \sum_{\ell=1}^{N}|\ell)\right). \quad (24)$$

The normal mode $|\beta_0^{(k)})$ describes a vibration mainly localized on the central core and uniformly distributed over the periphery of the star. The corresponding phonon frequency shift is equal to $\delta\Omega_0^{(k)} = -(N+1)\alpha^{(k)}/N$. By contrast, the normal mode $|\beta_N^{(k)})$ refers to a vibration that is uniformly distributed over the whole network. It thus describes an overall move of the vibrations whose phonon frequency shift vanishes, i.e., $\delta\Omega_N^{(k)} = 0$. Note that in both cases, the spatial dependence of these modes results from the overlaps between the totally symmetric state occupied by the exciton that accompanies the phonons and the other symmetric state involved in the virtual transitions.

According to Eq. (22), the phonon frequencies are either red shifted or blue shifted depending on the nature of the exciton. A red shift is induced when the exciton occupies the state $k = N$ whereas a blue shift occurs when the exciton occupies the state $k = 0$. In fact, only the sign of the shift changes depending on whether the exciton lies in the state $k = 0$ or $k = N$ so that $\delta\Omega_q^{(0)} = -\delta\Omega_q^{(N)}$, $\forall q = 0, \ldots, N-1$.

When the exciton occupies the totally symmetric state $|\chi_0\rangle$, the size dependence of the phonon frequency shifts $\delta\Omega_q^{(0)}$ is shown in Fig. 5. For the normal mode $q = 0$ that is mainly localized on the central core of the star, the frequency shift increases with both the size of the star and the adiabaticity [Fig. 5(a)]. Note that $\delta\Omega_0^{(0)}$ is proportional to the small polaron binding energy, as shown in Eq. (22). For instance, for $B = 0.01$, $\delta\Omega_0^{(0)}$ varies from $1.74 \times 10^{-2} E_B$ for $N = 10$ to $5.10 \times 10^{-2} E_B$ for $N = 100$. Similarly, for $N = 50$, $\delta\Omega_0^{(0)}$ increases from $3.62 \times 10^{-2} E_B$ for $B = 0.01$ to $1.13 \times 10^{-1} E_B$ for $B = 0.03$. A different behavior occurs for the shift $\delta\Omega_q^{(0)}$ of the extended normal modes $q = 1, \ldots, N-1$. First, this shift decreases with the size of the network [Fig. 5(b)]. Second, depending on the lattice size, it is approximately two or three orders of magnitude smaller than the shift experienced by the localized mode $q = 0$. Finally, $\delta\Omega_q^{(0)}$ is proportional to the small polaron binding energy and it increases with the adiabaticity. For instance, for $B = 0.01$, $\delta\Omega_q^{(0)}$ decreases from $1.59 \times 10^{-3} E_B$ for $N = 10$ to $5.01 \times 10^{-4} E_B$ for $N = 100$. Similarly, for $N = 50$, $\delta\Omega_q^{(0)}$ varies from $7.08 \times 10^{-4} E_B$ for $B = 0.01$ to $2.15 \times 10^{-2} E_B$ for $B = 0.03$.

The different features observed in Figs. 5 are easily explained when one considers the Taylor expansion of the shifts in the nonadiabatic limit. For small B_N values one obtains

$$\delta\Omega_0^{(0)} \approx \frac{N+1}{2\sqrt{N}} E_B B$$
$$\delta\Omega_q^{(0)} \approx \frac{E_B B}{8\sqrt{N}} \quad \forall q = 1, \ldots, N-1. \quad (25)$$

Provided that N is sufficiently important, these equations reveals that $\delta\Omega_0^{(0)} \propto E_B B_N$ whereas $\delta\Omega_q^{(0)} \propto E_B B_N/N$. Under this form, the N dependence of the shifts can be explained by drawing a parallel between the star graph and the linear chain. Indeed, a detailed analysis of the exciton-phonon system in a finite chain have revealed that the typical value of the phonon frequency shift can be expanded in a Taylor series as $\delta\Omega_{\rm typ} \propto E_B(\Delta\epsilon/\Omega_0)^\nu/L$ (see the results in Refs. [45–48]). In this expression, $\Delta\epsilon$ is the typical Bohr frequency of the virtual excitonic transitions responsible for the dressing of the phonons, E_B measures the strength of the exciton-phonon interaction, L denotes the extension of the phonon normal mode and ν is an exponent that governs the order of the expansion. In a linear chain with N sites, the phonons extend over the whole lattice and the typical Bohr frequency of the virtual excitonic transitions is approximately equal to 2Φ. As a result, to first order ($\nu = 1$), the phonon frequency shift scales as $\delta\Omega_{\rm typ} \propto E_B B/N$ [45–48].

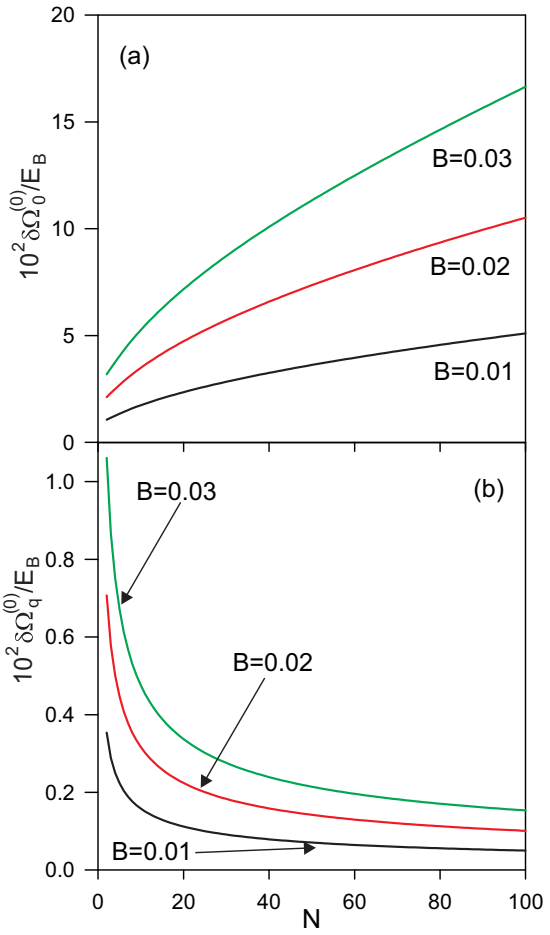

FIG. 5. Size dependence of the phonon frequency shift $\delta\Omega_q^{(0)}$ when the exciton occupies the totally symmetric state $|\chi_0\rangle$ for $C = 0.01$ and for $B = 0.01$, $B = 0.02$, and $B = 0.03$. (a) Shift that characterizes the phonon normal mode $q = 0$. (b) Shift that characterizes the phonon normal mode $q = 1, \ldots, N-1$.

In the star graph, the phonon normal modes $q = 1, \ldots, N-1$ defining Bloch waves delocalized over the periphery of the star, they behave as the vibrations that propagate in a linear chain. However, in that case, the typical Bohr frequency of the virtual excitonic transitions is about $\Delta\epsilon = 2\sqrt{N}\Phi$. Consequently, by analogy with what happens in the chain, the phonons on the star graph experience a similar shift, but with the correspondence $B \to B_N$. One thus obtains

$\delta\Omega_{\rm typ} \propto E_B B_N/N$. By contrast, the normal mode $q = 0$ refers to vibrations that are mainly localized on the central core of the network. Its extension thus reduces to unity giving rise to the disappearance of the factor $1/N$ in the expression of the corresponding frequency shift approximately equal to $\delta\Omega_{\rm typ} \propto E_B B_N$.

2. *Phonons dressed by an exciton occupying a Bloch state*

When the phonons are accompanied by an exciton that occupies a Bloch state $|\chi_k\rangle$ with $k = 1, \ldots, N-1$, the only elements of the phonon hopping constant matrix that contribute to the phonon dynamics are expressed as

$$\Lambda^{(k)}_{\ell\ell'} = \delta\Omega(\chi^*_{k\ell}\chi_{k\ell'} - \chi^*_{k\ell'}\chi_{k\ell}) \ \forall \ell \neq \ell' \neq 0, \qquad (26)$$

where the parameter $\delta\Omega$ is defined as

$$\delta\Omega = \frac{E_B B^2}{4 - B_N^2}. \qquad (27)$$

According to Eq. (26), the phonon hopping constant matrix connects each site of the periphery to the others, but it lets the core site isolated from the other sites. As previously, it is invariant under the discrete rotation of angle $\theta_0 = 2\pi/N$ and centered on the core site $\ell = 0$ so that it can be diagonalized by using the Bloch representation. In the context, it is straightforward to show that $\Lambda^{(k)}$ supports two kinds of eigenstates. First, since the core site is disconnected from the periphery, it exhibits an eigenstate $|\beta^{(k)}_0\rangle = |\ell = 0\rangle$ that is localized on the central core of the star graph. The frequency of this localized normal mode is equal to Ω_0 and it does not support any shift, i.e., $\delta\Omega^{(k)}_0 = 0$. Then, the phonon hopping constant matrix exhibits N normal modes that correspond to N Bloch vectors $|\beta^{(k)}_q\rangle = |\psi_q\rangle$, with $q = 1, \ldots, N$. These modes describe delocalized vibrations able to propagate along the periphery of the star, only. This spatial dependence originates in the overlaps between the Bloch state occupied by the exciton that accompanies the phonons and the remaining states that participate to the virtual transitions responsible for the dressing mechanism. However, only two normal modes experience a frequency shift, namely the modes $q = k$ and $q = N - k$, respectively. Note that the spatial dependence of these modes basically matches that of the excitonic wave function $\chi_{k\ell}$. The shift, defined as $\delta\Omega^{(k)}_q = \delta\Omega(\delta_{q,N-k} - \delta_{q,k})$, reveals that the frequency of the mode $q = k$ is red shifted whereas that of the mode $q = N - k$ is blue shifted.

The size dependence of the phonon frequency shifts $\delta\Omega$ is shown in Fig. 6. The frequency shift increases with the adiabaticity but it is clearly almost independent on the size of the network. Note that $\delta\Omega$ is proportional to the small polaron binding energy, as shown in Eq. (27). For instance, for $B = 0.02$, $\delta\Omega$ varies from $1.00 \times 10^{-2} E_B$ for $N = 10$ to $1.01 \times 10^{-2} E_B$ for $N = 100$. Similarly, for $N = 50$, $\delta\Omega$ increases from $2.50 \times 10^{-3} E_B$ for $B = 0.01$ to $2.28 \times 10^{-2} E_B$ for $B = 0.03$. Note that depending on the lattice size, the shift $\delta\Omega$ is approximately two orders of magnitude smaller than the shift experienced by the frequency of the phonons accompanied by an exciton in a totally symmetric state.

The behavior displayed in Fig. 6 can be interpreted by considering the Taylor expansion of the shift $\delta\Omega$ in the nonadiabatic limit, that is $\delta\Omega \approx E_B B^2/4$. In a marked contrast

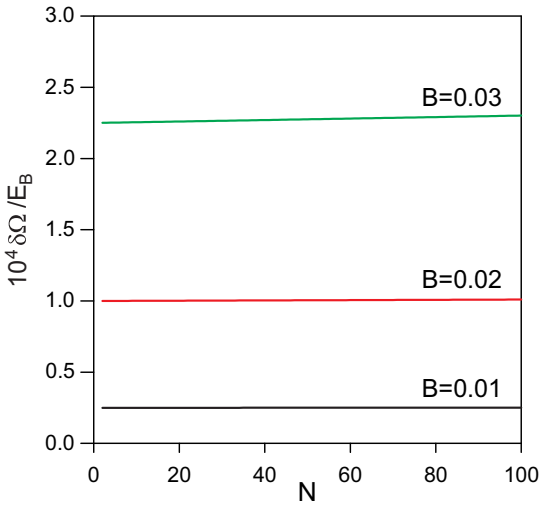

FIG. 6. Size dependence of the phonon frequency shift $\delta\Omega$ when the exciton occupies a Bloch state $k = 1, \ldots, N-1$ for $C = 0.01$ and for $B = 0.01$, $B = 0.02$, and $B = 0.03$.

with what happens when the exciton occupies a totally symmetric state, one obtains a phonon frequency shift that is N independent and that depends quadratically on the adiabaticity B. These two surprising features can be understood as follows. Indeed, still by drawing a parallel between the star graph and the linear chain, the normal modes $q = 1, \ldots, N$ characterize extended phonons that propagate over the periphery of the star. Therefore, since the typical Bohr frequency of the virtual excitonic transitions is about $\Delta\epsilon = 2\sqrt{N}\Phi$, the typical value of the phonon frequency shift scales as $\delta\Omega_{\rm typ} \propto E_B (B_N)^\nu/N$. The key point here results from the fact that the exciton occupies a Bloch state. In that case, the virtual transitions towards the totally symmetric state $|\chi_0\rangle$ are exactly compensated by those towards the totally symmetric state $|\chi_N\rangle$. Consequently, the first-order contribution of the phonon frequency shift with respect to the exciton Bohr frequency vanishes. One thus obtains $\nu = 2$ that gives rise to an N-independent phonon frequency shift that scales as B^2. Note that in addition to the extended normal modes, we have shown that the star graph supports a mode $q = 0$ localized on the core site. Since the exciton occupies a Bloch states confined to the periphery of the graph, the exciton-phonon interaction vanishes resulting in a zero frequency shift for this localized phonon mode.

To conclude this section, let us mention that a careful reading of Eq. (26) reveals that the phonon hopping constant matrix vanishes for real values of the exciton wave functions. However, the Bloch states are eigenstates associated to a $(N-1)$-fold degenerate energy level. Therefore, any superimposition of Bloch states remaining an eigenstate, it is straightforward to build a set of real excitonic wave functions. An example among many is given by the set of excitonic states $|\Psi^{(1)}_\ell\rangle = (|1\rangle - |\ell\rangle)/\sqrt{2}$ for $\ell = 2, \ldots, N$. Consequently, when the exciton occupies such a state, it does not induce any phonon frequency shift.

IV. CONCLUSION

In this paper, we have introduced a microscopic model for describing an exciton coupled with optical phonons on a

star graph. Within the nonadiabatic weak-coupling limit, the properties of the exciton-phonon system was studied using the operatorial formulation of the quasidegenerate perturbation theory. This method provides a new point of view in which the dynamics is governed by an effective Hamiltonian that does no longer characterize independent excitations but accounts for exciton-phonon entanglement. The exciton is dressed by a virtual phonon cloud whereas the phonons are clothed by virtual excitonic transitions.

In accordance with the standard polaron concept, the dressing of the exciton favors two main effects. First, it yields a red shift of the energy of each excitonic local state. Then, it modifies the propagation of the exciton that delocalizes according to a reduced hopping constant. Consequently, it has been shown that the graph exhibits a $(N-1)$-fold degenerate eigenenergy associated to $N-1$ excitonic states delocalized over the periphery of the star. Although the dressing preserves the degeneracy, it induces a red shift of this degenerate energy level approximately equal to the so-called small polaron binding energy. In addition, the graph supports two totally symmetric eigenstates both localized on the central core and uniformly distributed over the periphery. These states define two discrete energy levels located on each side of the degenerate eigenenergy. Owing to the dressing, these energy levels experience a shift that originates in both the red shift of each excitonic local state and the band-narrowing effect induced by the decay of the exciton hopping constant.

Similarly, we have shown that the influence of an exciton that dresses the phonons is twofold. First, it induces a shift of the frequency of each local oscillator. Then, it provides couplings between distinct local oscillators that specifies pathways for the phonon propagation whose nature is intimately connected to the overlaps between the excitonic wave functions involved in the virtual transitions that dress the phonons. Therefore, the motion of the exciton confers the ability of the dressed phonons to propagate over the graph so that the corresponding normal modes are fundamentally different from the localized normal modes associated to free phonons. The key point is that the nature of the dressed normal modes depends on the state occupied by the exciton that accompanies the phonons. When the exciton lies in a totally symmetric state, three kinds of normal modes occur. First, the graph exhibits $N-1$ normal modes that correspond to vibrational plane waves delocalized over the periphery of the star. Then, it supports a vibration mainly localized on the central core and uniformly distributed over the periphery. Finally, it shows a normal mode uniformly distributed over the whole network that corresponds to an overall move of the vibrations. When the exciton occupies a degenerate Bloch state, two kinds of normal modes occur. Indeed, the graph supports N normal modes fully delocalized over the periphery of the star and a single mode localized only on the central core.

In all the previous situations, we have characterized the behavior of the phonon frequencies with respect to the relevant parameters of the model. In particular, it has been shown that these frequencies are either red shifted or blue shifted, depending on the nature of the dressing mechanism. Some of them increase as the size of the graph increases whereas others decrease with the star size.

Finally, with the objective of revisiting the concept of dissipative quantum walk on complex networks, the present study will serve as a starting point for investigating the quantum decoherence that inherently affects the dynamics of an excitonic qubit moving on a star graph. A qubit corresponding to a superimposition between the vacuum and a one-exciton state, the decoherence will result from the fact that the phonons evolve differently depending on whether the exciton is present or absent. The way the coherence disappears is thus intimately related to the behavior of the phonons frequencies shifts [45,46]. Therefore, its knowledge will provide a clear understanding on the behavior of the decoherence rate with respect to the model parameter in general and with the size of the graph, in particular.

ACKNOWLEDGMENTS

The authors would like to gratefully acknowledge Professor E. de Prunelé for fruitful discussions.

APPENDIX: QUASIDEGENERATE SECOND-ORDER PERTURBATION THEORY

The quasidegenerate PT involves a unitary transformation $U=\exp(S)$ that yields a block-diagonal transformed Hamiltonian $\hat{H}=UHU^{\dagger}$ in the unperturbed basis $|\chi_k\rangle\otimes|\{n_\ell\}\rangle$. The only restriction is that the desired Hamiltonian must conserve the phonon number. To proceed, any operator O acting in $\mathcal{E}$ can be split as $O=O_C+O_{NC}$, where O_C is the phonon conserving part whereas O_{NC} is the phonon nonconserving part. In that context, because $V_C=0$, one seeks the anti-Hermitian generator $S\equiv S_{NC}$ as a phonon nonconserving operator. It is expanded as a Taylor series as $S=S_1+S_2+\ldots$ where S_q is the qth order correction in the coupling V. Consequently, $\hat{H}$ becomes

$$\hat{H}=H_0+V+[S_1,H_0]+[S_1,V]+[S_2,H_0]+\tfrac{1}{2}\{S_1,[S_1,H_0]\}+\ldots. \tag{A1}$$

From Eq. (A1), S is derived order by order to obtain a block-diagonal form for $\hat{H}$ at the desired order. Up to second order, the solution is given by the equations

$$\begin{aligned}[H_0,S_1]&=V_{NC}\\ [H_0,S_2]&=\tfrac{1}{2}[S_1,V]_{NC}\\ \hat{H}&=H_0+\tfrac{1}{2}[S_1,V]_C.\end{aligned} \tag{A2}$$

Because V is a linear combination of the phonon operators, one seeks $S_1=\sum_{\ell=0}^{N}Z^{(\ell)}a_\ell^{\dagger}-Z^{(\ell)\dagger}a_\ell$ where the unknown operator $Z^{(\ell)}$ acts in $\mathcal{E}_A$, only. Inserting this expression into Eq. (A2) yields $Z^{(\ell)}_{kk'}=M^{(\ell)}_{kk'}/(\epsilon_k-\epsilon_{k'}+\Omega_0)$. The knowledge of S_1 allows us to compute the commutator $[S_1,V]$ that is required to derive both $\hat{H}$ and S_2. This commutator is defined as

$$\frac{1}{2}[S_1,V]=\sum_{\ell\ell'}A^{(\ell\ell')}a_\ell^{\dagger}a_{\ell'}^{\dagger}+A^{(\ell\ell')\dagger}a_{\ell'}a_\ell+\sum_{\ell\ell'}A^{(\ell\ell')}a_\ell^{\dagger}a_{\ell'}+A^{(\ell\ell')\dagger}a_{\ell'}^{\dagger}a_\ell+\sum_{\ell}C^{(\ell)}, \tag{A3}$$

where $C^{(\ell)} = -(Z^{(\ell)\dagger}M^{(\ell)} + M^{(\ell)}Z^{(\ell)})/2$ and $A^{(\ell\ell')} = [Z^{(\ell)}, M^{(\ell')}]/2$. From the phonon conserving part of Eq. (A3), $\hat{H}$ becomes

$$\hat{H} = H_A + \sum_{\ell} C^{(\ell)} + \sum_{\ell\ell'} (\Omega_0 \delta_{\ell\ell'} + A^{(\ell\ell')} + A^{(\ell'\ell)\dagger}) a_{\ell}^{\dagger} a_{\ell'}. \tag{A4}$$

We thus recover Eq. (8) with $\delta H_A = \sum_{\ell} C^{(\ell)}$ and $\Lambda(\ell\ell') = A^{(\ell\ell')} + A^{(\ell'\ell)\dagger}$ whose representation in the unperturbed basis yields Eq. (9). From the nondiagonal part of Eq. (A3), one seeks S_2 as

$$S_2 = \sum_{\ell\ell'} E^{(\ell\ell')} a_{\ell}^{\dagger} a_{\ell'}^{\dagger} - E^{(\ell\ell')\dagger} a_{\ell'} a_{\ell}. \tag{A5}$$

The unknown operators $E^{(\ell\ell')}$ acts in $\mathcal{E}_A$, only. Inserting this expression into Eq. (A2) yields $E_{kk'}^{(\ell\ell')} = A_{kk'}^{(\ell\ell')}/(\epsilon_k - \epsilon_{k'} + 2\Omega_0)$.

[1] O. Mulken and A. Blumen, Phys. Rep. **502**, 37 (2011).
[2] D. Astruc, E. Boisselier, and C. Ornelas, Chem. Rev. **110**, 1857 (2010).
[3] O. Mulken, V. Bierbaun, and A. Blumen, J. Chem. Phys. **124**, 124905 (2006).
[4] A. M. Childs, Phys. Rev. Lett. **102**, 180501 (2009).
[5] E. Farhi, J. Goldstone, and S. Gutmann, Theory Comput. **4**, 169 (2008).
[6] A. M. Childs, E. Farhi, and S. Gutmann, Quant. Info. Proc. **1**, 35 (2002).
[7] E. Farhi and S. Gutmann, Phys. Rev. A **57**, 2403 (1998).
[8] A. M. Childs and J. Goldstone, Phys. Rev. A **70**, 022314 (2004).
[9] L. K. Grover, Phys. Rev. Lett. **79**, 325 (1997).
[10] V. Pouhtier, J. Chem. Phys. **139**, 234111 (2013).
[11] V. Pouthier, Phys. Rev. E **90**, 022818 (2014).
[12] P. Rebentrost, M. Mohseni, I. Kassal, S. Lloyd, and A. Aspuru-Guzik, New J. Phys. **11**, 033003 (2009).
[13] S. R. Jackson, T. J. Khoo, and F. W. Strauch, Phys. Rev. A **86**, 022335 (2012).
[14] A. L. Cardoso, R. F. S. Andrade, and A. M. C. Souza, Phys. Rev. B **78**, 214202 (2008).
[15] X. P. Xu, W. Li, and F. Liu, Phys. Rev. E **78**, 052103 (2008).
[16] Z. Darazs, A. Anishchenko, T. Kiss, A. Blumen, and O. Mulken, Phys. Rev. E **90**, 032113 (2014).
[17] E. Agliari, A. Blumen, and O. Mulken, Phys. Rev. A **82**, 012305 (2010).
[18] O. Mulken, M. Dolgushev, and M. Galiceanu, Phys. Rev. E **93**, 022304 (2016).
[19] S. Salimi, Ann. Phys. (N.Y.) **324**, 1185 (2009).
[20] X. P. Xu, J. Phys. A **42**, 115205 (2009).
[21] A. Ziletti, F. Borgonovi, G. L. Celardo, F. M. Izrailev, L. Kaplan, and V. G. Zelevinsky, Phys. Rev. B **85**, 052201 (2012).
[22] A. Anishchenko, A. Blumen, and O. Mulken, Quant. Info. Proc. **11**, 1273 (2012).
[23] V. Pouthier, Quant. Info. Proc. **14**, 491 (2015).
[24] V. Pouthier, Quant. Info. Proc. **14**, 3139 (2015).
[25] C. H. Bennet and D. P. DiVincenzo, Nature (London) **404**, 247 (2000).
[26] S. Bose, Phys. Rev. Lett. **91**, 207901 (2003).
[27] S. Bose, Contemp. Phys. **48**, 13 (2007).
[28] M. Christandl, N. Datta, A. Ekert, and A. J. Landahl, Phys. Rev. Lett. **92**, 187902 (2004).
[29] M. Christandl, N. Datta, T. C. Dorlas, A. Ekert, A. Kay, and A. J. Landahl, Phys. Rev. A **71**, 032312 (2005).
[30] A. Ajoy and P. Cappellaro, Phys. Rev. A **85**, 042305 (2012).
[31] D. Burgarth and S. Bose, Phys. Rev. A **71**, 052315 (2005).
[32] D. Burgarth, Eur. Phys. J. Special Topics **151**, 147 (2007).
[33] M. B. Plenio, J. Hartley, and J. Eisert, New J. Phys. **6**, 36 (2004).
[34] M. B. Plenio and F. L. Semio, New J. Phys. **7**, 73 (2005).
[35] C. Gollub, Ph.D. thesis, Ludwig Maximilian University of Munich, 2009 (unpublished).
[36] V. Pouthier, Phys. Rev. B **85**, 214303 (2012).
[37] V. Pouthier, J. Phys. Condens. Matter **24**, 445401 (2012).
[38] E. Joos, H. D. Zeh, C. Kiefer, D. Giulini, J. Kupsch, and I. O. Stamatescu, *Decoherence and the Appearance of a Classical World in Quantum Theory* (Springer, New York, 2003).
[39] M. Schlosshauer, *Decoherence and the Quantum-to-Classical Transition* (Springer Verlag, Berlin, 2007).
[40] H. P. Breuer and F. Petruccione, *The Theory of Open Quantum Systems* (Oxford University Press, New York, 2007).
[41] S. M. Barnett and S. Stenholm, Phys. Rev. A **64**, 033808 (2001).
[42] V. Pouthier, J. Phys. Condens. Matter **22**, 255601 (2010).
[43] M. Esposito and P. Gaspard, Phys. Rev. E **68**, 066112 (2003).
[44] V. Pouthier, J. Phys. Condens. Matter **22**, 385401 (2010).
[45] V. Pouthier, Phys. Rev. B **83**, 085418 (2011).
[46] V. Pouthier, J. Chem. Phys. **134**, 114516 (2011).
[47] V. Pouthier, Phys. Rev. B **84**, 134301 (2011).
[48] V. Pouthier, J. Chem. Phys. **138**, 044108 (2013).
[49] T. Holstein, Ann. Phys. (N.Y.) **8**, 325 (1959); **8**, 343 (1959).
[50] V. May and O. Kuhn, *Charge and Energy Transfer Dynamics in Molecular Systems* (Wiley-VCH Verlag, Berlin, 2000).
[51] M. Wagner, *Unitary Transformations in Solid State Physics* (North-Holland, Amsterdam, 1986).
[52] C. Cohen-Tannoudji, J. Dupont-Roc, and G. Grynberg, *Atoms-Photon Interactions: Basic Processes and Applications* (Wiley, New York, 1992).
[53] D. Cevizovic, S. Zekovic, and Z. Ivic, Chem. Phys. Lett. **480**, 75 (2009).
[54] A. S. Alexandrov and J. T. Devreese, *Advances in Polaron Physics* (Springer Verlag, Berlin, 2010).